Powder Technology 258 (2014) 331–343

Contents lists available at ScienceDirect

Powder Technology

journal homepage: www.elsevier.com/locate/powtec

Design and development of solid nanoparticulate dosage forms of telmisartan for bioavailability enhancement by integration of experimental design and principal component analysis

Jaydeep Patel [a,*], Anjali Dhingani [a], Kevin Garala [a], Mihir Raval [b], Navin Sheth [b]

[a] Atmiya Institute of Pharmacy, Kalawad Road, Rajkot 360005, Gujarat, India
[b] Department of Pharmaceutical Sciences, Saurashtra University, Rajkot 360005, Gujarat, India

ARTICLE INFO

Article history:
Received 11 June 2013
Received in revised form 18 February 2014
Accepted 1 March 2014
Available online 11 March 2014

Keywords:
Bioavailability
Nanosuspension
Nanocrystals
Principal component analysis
Quality by design
Telmisartan

ABSTRACT

Aim of the present investigation was to develop nanoparticulate solid oral dosage forms of a poorly water soluble antihypertensive agent, telmisartan (TLM) by converting the optimized batch of drug loaded nanosuspensions into a tablet dosage form using lyophilization technique. The TLM loaded nanosuspensions were optimized by implementation of 3^2 full factorial design along with principal component analysis (PCA) with concentration of stabilizer and amount of milling agents as factors. The optimized batch of TLM loaded nanosuspension exhibited a mean particle size of 334.67 ± 10.43 nm. The results of various instrumental techniques illustrated retention of drug crystallinity after milling and lyophilization. The results of in vitro drug release study of tablets containing drug nanocrystals revealed remarkable improvement in the dissolution rate as compared to the marketed tablet (Sartel® 20). The results of in vivo pharmacokinetic study on Wister rats revealed 1.5-fold enhancement in oral bioavailability for tablets containing TLM nanocrystals against the marketed tablets. The present study proposed nanosuspension as a suitable approach for developing nanosized solid oral dosage forms of poorly water soluble drugs like telmisartan using design of experiment and principal component analysis as two important paradigms of quality by design technique.

1. Introduction

Oral drug delivery is a preferred route for drug administration as it avoids pain and risk of infection associated with parenteral administration and thereby leads to greater patient compliance. However, oral administration of many drugs results in lower absorption which is generally attributed to poor aqueous solubility, poor membrane permeation and efflux by P-glycoprotein (P-gp) [1]. Aqueous solubility of an orally administered drug is a critical determinant since the drug becomes available for absorption at specific sites within the GI tract only after its dissolution in GI fluid. Typically, these drugs have low oral bioavailability, erratic absorption, large inter and intrasubject variability and lack of dose proportionality [2,3]. Telmisartan (TLM) is the most widely prescribed selective antagonists of angiotensin II type-1 receptor (AT_1R) for the treatment of essential hypertension [4,5]. However, high lipophilicity and practical insolubility in water renders it a class II drug in the biopharmaceutical classification system which might be the reason for its slow or incomplete dissolution in the GI tract along with poor oral bioavailability (42%). Solubility enhancement approaches such as solid dispersion [6,7] and inclusion complexation [8] have already been investigated for the improvement of oral efficacy of TLM. However, none of these approaches offered an adequate improvement in therapeutic potential due to the limitations of the dosage form itself.

Nanotechnology is a technique which reduces the particle size of drug molecules down to the sub-micron range. This is a prevalent practice in the pharmaceutical field especially for the delivery of poorly water soluble drugs. Nanosuspensions are colloidal dispersions of nanosized drug particles (nanocrystals) stabilized by surfactants. The high phase stability of nanocrystals offers a potential benefit against the most commonly employed formulation technologies for poorly soluble drugs. Apart from this, drug nanocrystals not only increase dissolution velocity but also increase saturation solubility and hence they can improve the oral absorption of poorly soluble drugs, more efficiently [9–11]. The Quality by Design (QbD) paradigm underlying pharmaceutical drug product development relies on multivariate data, both from formulation and the process in order to explain the multi-factorial relationship between formulation variables, process variables and drug product attributes [12]. Design of experiments (DoE), risk assessment, principal component analysis (PCA) and process analytical technology (PAT) are the major tools that can be used in the QbD process as and when necessary [13]. The majority of scientists now routinely use DoE in order to reduce costs, improve quality within timelines to obtain robust products and processes. In light of these, the aim of the present investigation was to design and develop novel nanoparticulate solid oral dosage forms of TLM using design of experiment and PCA.

* Corresponding author. Tel.: +91 9624801807; fax: +91 281 2585083.
E-mail address: jmpatel7@gmail.com (J. Patel).

http://dx.doi.org/10.1016/j.powtec.2014.03.001
0032-5910/

2. Materials and methods

2.1. Materials

Telmisartan was obtained as a gift sample from Torrent Research Center, Gandhinagar, India. The materials; hydroxy propyl methyl cellulose (HPMC) E5 and hydroxy propyl cellulose (HPC) (klucel LF) were donated by Colorcon, Goa, India. Zirconia and glass milling beads were purchased from BioSpec Inc., Bartlesville, OK, USA. Cryoprotectants such as glucose, mannitol, trehalose and sucrose were purchased from S.D. Fine Chem, Mumbai, India. Stabilizers such as poloxamer 188, poloxamer 407, polyvinyl alcohol (PVA), polyvinyl pyrrolidine (PVP) K30 and sodium lauryl sulfate (SLS) were purchased from Himedia Labs, Mumbai, India. Microcrystalline cellulose (MCC) PH 200, sodium starch glycollate (SSG), magnesium stearate and talc were procured from Loba Chem, Mumbai, India. Acetonitrile and methanol used in the present study were of high performance liquid chromatography (HPLC) grade. Double distilled water was used throughout the study.

2.2. Formulation and development of drug loaded nanosuspensions

2.2.1. Preparation of drug loaded nanosuspensions

A wide mouth glass vial (outside diameter of 2.5 cm, inside diameter of 2.2 cm and inside depth of 5.2 cm with total volume 10 mL) was exploited to mimic a media milling machine. The total volume of the slurry (drug, stabilizer and water) was 5 mL which was considered as the batch size [14]. Subsequently each batch was charged with milling agents and exposed to stirring at fixed speed using a magnetic stirrer (Remi Laboratory Instruments, Mumbai, India) for preset time periods. At the end of the process each system was filtered through a membrane filter (0.45 μm) and the milled suspension (filtrate) was combined with rinsing of beads and vessel. The samples were stored at refrigerated conditions (2–8 °C) in screw capped glass vials until further use [15–17].

2.2.2. Preparation of drug loaded coarse suspensions

Drug powder was grounded in a mortar for 10 min and dispersed in 1% w/w of stabilizer solutions with a drug load of 5% w/w. The obtained suspension was sonicated in an ultrasonic water bath (Frontline FS-4, Mumbai, India) for 20 min and stored at refrigerated conditions (2–8 °C) in screw capped glass vials until further use [18].

2.2.3. Preliminary optimization of formulation parameters

TLM loaded nanosuspensions were optimized exclusively for factors like type of milling agents, type of stabilizer, concentration of drug, size of milling agents, ratio of drug to stabilizer, amount of milling media, stirring time and stirring speed as contributing factors by one variable at one time (OVAT) approach, keeping others constant [19,20]. Each batch was repeated thrice for the confirmation of reproducibility.

2.2.4. Experimental design

Based on preliminary trials the outcome of critical factors like amount of milling agent and drug to stabilizer ratio on the properties of TLM loaded nanosuspensions were evaluated by implementing 3^2 full factorial design along with principal component analysis (PCA) [21,22]. Critical responses were identified by PCA using a trial version of Unscrambler® 10.2 (CAMO AS, Norway, Switzerland). The data for all experimental design batches of drug loaded nanosuspensions were utilized to construct loading plot, scoring plot, agglomerative hierarchy cluster analysis (AHCA) plot, correlation loading plot and scree plot by PCA [23,24]. The experimental design consisted of a total of 9 runs (TLM-NS-F1 to TLM-NS-F9) and each of them was formulated in triplicates in order to estimate reproducibility of the model (Table 1). A second order quadratic model incorporating interactive and polynomial terms was used to evaluate the responses.

Table 1
Design layout of 3^2 full factorial design batches for TLM loaded nanosuspensions.

Batch code	Transformed values	
	X_1[a]	X_2[b]
TLM-NS-F1	−1	−1
TLM-NS-F2	−1	0
TLM-NS-F3	−1	1
TLM-NS-F4	0	−1
TLM-NS-F5	0	0
TLM-NS-F6	0	1
TLM-NS-F7	1	−1
TLM-NS-F8	1	0
TLM-NS-F9	1	1
Coded values	Actual values	
	X_1[a]	X_2[b]
−1	0.5	1
0	0.75	3
1	1	5

[a] X_1 — Concentration of stabilizer (% w/v).
[b] X_2 — Amount of milling agents (g).

$$Y_i = b_0 + b_1X_1 + b_2X_2 + b_3X_3 + b_{12}X_1X_2 + b_{23}X_2X_3 + b_{13}X_1X_3 + b_{11}{X_1}^2 + b_{22}{X_2}^2 + b_{33}{X_3}^2 \quad (1)$$

where, Y_i was dependent variable, b_0 was arithmetic mean of nine runs and b_i was the estimated coefficient for factor X_i. The main effects (X_1, X_2 and X_3) signify average result of altering one factor at a time from its lowest to highest value whereas the interaction terms (X_1X_2, X_2X_3 and X_1X_3) prompt change in responses when two factors were simultaneously altered. The polynomial terms (X_1^2, X_2^2 and X_3^2) were added to investigate nonlinearity of the model [25]. Data were further analyzed by Microsoft Excel® version 2010 (Microsoft Corporation, Washington, USA) for regression analysis. Analysis of variance (ANOVA) study was used to assure nonsignificant difference between the developed full model and the reduced model. Contour, response surface and perturbation plots were generated to study response variations against independent variables using Statistica® 8 (StatSoft Inc. Oklahoma, USA) and Design Expert® 8.0.7.1 (Stat-Ease, Inc. Minneapolis, USA) software. Additionally, the composition of the optimized (check point) batch was derived by constructing overlay plots. The percentage relative error of each response was calculated using the following equation in order to judge validity of the model [26].

$$\%\text{Relative Error} = \frac{|\text{Predicted value-Experimental value}|}{\text{Predicted value}} \times 100. \quad (2)$$

2.2.5. Evaluation parameters for drug loaded nanosuspensions

2.2.5.1. Particle size and size distribution. The particle size and its distribution (polydispersibility index — PI) were measured for all batches of TLM loaded nanosuspensions by particle size analyzer (Zetatrac, U2552, New York, USA). For each sample a drop of nanosuspension (about 50 μL) was diluted with 5 mL purified water. All samples were subjected to a brief period of sonication (15–30 s) prior to size analysis with the intention to disperse any aggregates if present. The particle size and PI were recorded in triplicates at 25 °C [27,28].

2.2.5.2. Saturation solubility. For all experimental design batches of TLM loaded nanosuspensions, saturation solubilities were determined by shake-flask method. Surplus amount of samples were added individually to volumetric flasks (250 mL), each containing 100 mL of distilled

water. The samples were subsequently charged into an environmental shaker bath (Tempo Instruments and Equipments Pvt. Ltd., Mumbai, India) for a period of 72 h at 37 °C temperature and 300 rpm speed. After an additional equilibrium for 72 h, samples were subjected to centrifugation for 10 min at 10,000 rpm (Remi Laboratory Instruments, Mumbai, India). The supernatant of each sample was filtered through a membrane filter (0.45 μm) to isolate any undissolved drug if present. The filtrate from each sample was suitably diluted and their drug content was estimated by spectrophotometric method against blank using a double beam UV–Visible spectrophotometer (Pharmaspec-1700, Shimadzu Corporation, Tokyo, Japan) [28].

2.2.5.3. Zeta potential (ζ). Zeta potentials were assessed for all the batches of experimental design for TLM loaded nanosuspensions by determining the particle electrophoretic mobility using particle size analyzer introduced in Section 2.2.5.1. The method employed for sample preparation was similar to that of particle size measurement as elaborated in Section 2.2.5.1. The measurements were performed in purified water (pH 5.5–6.0) adjusted to a standardized conductivity of 50 μS/cm with sodium chloride solution (0.9% w/v) in water to avoid changes in ζ values due to day-to-day variations in conductivity of water. The mean values of ζ for three independent samples were documented [29].

2.2.5.4. In vitro drug release. The in vitro drug release studies for all the experimental design batches of TLM loaded nanosuspensions and coarse suspension were conducted by USP type II (paddle type) dissolution apparatus (TDT 06P, Electrolab, Mumbai, India) containing 900 mL of 0.1 M HCl. The dissolution medium was continuously maintained at 37 ± 0.5 °C with a stirring speed of 50 rpm. At predetermined time intervals up to 90 min, 5 mL of samples was withdrawn and immediately filtered through 0.45 μm membrane filters. Equal volumes of respective fresh dissolution medium were used for the replacement of samples withdrawn. The amount of drug dissolved was determined spectrophotometrically after suitable dilution of the samples against blank. On the basis of in vitro release profiles parameters like % dissolution efficiency at 10 min ($\%DE_{10\ min}$), mean dissolution time (MDT), dissimilarity factor (f_1) and similarity factor (f_2) were calculated for comparison purposes [30–33].

2.2.5.5. Transmission electron microscopy (TEM). The optimized batch of TLM loaded nanosuspension was subjected to transmission electron microscope (H-7000, Hitachi, Ibaraki, Japan) in order to estimate its particle morphology. The formulation was diluted (1000 times) with purified water and plunged for 10–15 min on a coated carbon grid stained with 2% uranyl acetate solution. The sample was subsequently washed with fresh distilled water before analysis. Radiation generated at 200 kV was utilized as X-ray source with camera length of 100 cm. Two dimensions of X-ray patterns were photographed [34].

2.2.5.6. Short term physical stability. The physical stability of the optimized batch of TLM loaded nanosuspension was evaluated over a period of one week at 25 °C in glass vials. After a period of 7 days, aliquots of TLM loaded nanosuspension were subjected to the determination of particle size, PI, ζ and saturation solubility in triplicates to evaluate its potential for solid dosage form conversion by lyophilization [19].

2.2.6. Formulation and development of drug nanocrystals

2.2.6.1. Preparation of drug nanocrystals by lyophilization. With an objective to provide long-term stability, the optimized batch of TLM loaded nanosuspension was subjected to lyophilization. Five different cryoprotectants (mannitol, lactose, glucose, sucrose and trehalose) at four different concentrations (1%, 2.5%, 5% and 10% w/v) were utilized for this purpose. Briefly, about 2 mL of freshly prepared optimized batch of TLM loaded nanosuspension was transferred into 10 mL glass vials containing cryoprotectant. Each of these mixtures was oscillated until the cryoprotectant was dissolved completely by environmental shaker bath. All samples were frozen using a deep freeze (MDF-382E, Sanyo, Japan) at −80 °C for 24 h and lyophilized subsequently using a lyophilizer (Unitor 200, Virtis Equipment, Gardiner, New York, USA) at −40 °C temperature and 0.10 mbar pressure for a period of 48 h. The selection of type of cryoprotectant and its concentration was done on the basis of product appearance, color and ease of redispersibility by the scoring method [35].

2.2.6.2. Solid state characterization of lyophilized drug nanocrystals

2.2.6.2.1. Fourier transform infrared spectroscopy (FTIR). FTIR spectra of the optimized batch of lyophilized TLM nanocrystals and drug powder were recorded using a FTIR spectrophotometer (Nicolet iS10, Thermo Fisher Scientific Inc., USA). For recording of spectra, approximately 1 g of powder sample was placed on the sample holder and compressed lightly using a pressure clamp. Scanning was performed in the range of 4000–400 cm^{-1} [36,37].

2.2.6.2.2. Differential scanning calorimetry (DSC). The samples of optimized batch of lyophilized TLM nanocrystals and drug powder were subjected to differential scanning calorimeter (DSC-60, Shimadzu Corporation, Japan) which was previously calibrated with indium standard. Sample (~5–10 mg) was hermetically sealed in an aluminum crucible and subjected to a purging of nitrogen gas at a flow rate of 50 mL/min. The heating was done at 30–300 °C temperature and a rate of 10 °C/min [38,39].

2.2.6.2.3. Powder X-ray diffraction (PXRD). The crystalline nature of the optimized batch of lyophilized TLM nanocrystals and drug powder was determined using a powder X-ray diffractometer (Philips X'Pert MPD, Eindhoven, Netherlands) with Cu Kα radiation (λ = 1.5406 Å) against their drug powder sample. The tube voltage and amperes were set to 45 kV and 40 mA, respectively. The samples were scanned for 2θ ranging from 5 to 50° at a speed of ~0.01 2θ/s [40].

2.2.6.2.4. Scanning electron microscopy (SEM). The microscopic structures of the optimized batch of lyophilized TLM nanocrystals and drug powder were observed by scanning electron microscope (JSM-6380LV, JEOL, UK) with an acceleration voltage of 20 kV. The sample was fixed onto metal stubs using double-sided conductive tape which was previously secured on aluminum stubs and subsequently coated with gold under a vacuum before imaging (JEOL JFC-1600, Auto Fine Coater, JEOL, UK). The scale bar was calibrated accurately and images were captured from different locations [41].

2.2.6.3. Evaluation parameters for lyophilized drug nanocrystals

2.2.6.3.1. Particle size and size distribution. Particle size and size distribution of the optimized batch of lyophilized TLM nanocrystals (~50 mg) was determined after reconstitution with distilled water (~5 mL) using the particle size analyzer mentioned earlier in Section 2.2.5.1. The study was repeated in triplicates and their average values were documented [34,35].

2.2.6.3.2. Saturation solubility. The saturation solubility of optimized batch of lyophilized TLM nanocrystals was determined in triplicates by shake-flask method as mentioned earlier in Section 2.3.5.2. The study was repeated in triplicates and their average values were documented [32].

2.2.6.3.3. Zeta potential (ζ). The ζ values of the optimized batch of lyophilized TLM nanocrystals (~50 mg) were assessed by determining the particle electrophoretic mobility after its reconstitution in distilled water (~5 mL) using a similar process as stated earlier in Section 2.2.5.3. The study was performed in triplicate in order to estimate reproducibility of the results [31,38].

2.2.6.3.4. Percentage drug content. Percentage drug content of the optimized batch of lyophilized TLM nanocrystals was determined by dissolving 100 mg of sample in 100 mL of methanol. The sample was centrifuged (5000 rpm, 10 min) and the supernatant was subjected to estimation of drug contents against blank using a double beam UV

spectrophotometer. The study was repeated in triplicates and the average values were documented [27,28].

2.2.6.3.5. In vitro drug release. The in vitro drug release patterns of the optimized batch of lyophilized TLM nanocrystals and drug powder were constructed by performing in vitro dissolution of each sample in '0' sized hard gelatin capsules (HGC) using USP type II dissolution apparatus containing 900 mL of 0.1 M HCl. All other test parameters were kept similar as mentioned earlier in Section 2.2.5.4 [36,42]. The study was repeated in triplicates in order to confirm reproducibility of the results. Parameters like DE, MDT, f_1 and f_2 were calculated for comparison purpose [30–33].

2.2.6.3.6. Stability study. The stability of optimized batch of lyophilized TLM nanocrystals was explored in screw capped glass vials at three different storage conditions viz; 4 ± 2 °C, 25 ± 2 °C and at 40 ± 2 °C for a period of 6 months. In order to estimate physical stability of TLM nanocrystals parameters like particle size, PI and ζ values were recorded at predetermined time intervals [31,32].

2.2.7. Formulation and development of drug nanocrystals loaded tablets

2.2.7.1. Preparation of drug nanocrystals loaded tablets. Accurately weighed amount of optimized TLM nanocrystals along with directly compressible diluent (MCC PH 200) was mixed by geometric dilution method [43]. To these mixtures, 5% w/w SSG as superdisintegrant, 2% w/w of magnesium stearate as lubricant and 1% w/w of talc as glidant were added and mixed further using a double cone blender (Dolphin, Mumbai, India) for a period of 3–5 min. Direct compression method was adopted for the preparation of TLM nanocrystals loaded tablets. Each powder blend was compacted into tablets using a rotary tablet compression machine (Mini Press-I, Rimek, India) fitted with 6 mm round, standard concave type B tooling with a compression force that provide acceptable tablet hardness. For comparison purpose conventional tablets (CT) were prepared [42].

2.2.7.2. Evaluation parameters for drug nanocrystals loaded tablets

2.2.7.2.1. Flowability of pre-compressed blends. Flow properties of ready for compression (RFC) blends of all batches of tablets containing TLM nanocrystals were evaluated by determining angle of repose, Carr's index (CI) and Hausner ratio (HR).

2.2.7.2.2. Physical characterization. TLM nanocrystals loaded tablets and conventional tablets were subjected to the estimation of physical parameters such as hardness, friability, disintegration, thickness, diameter and weight variation as per pharmacopoeial specifications [43].

2.2.7.2.3. Reconstitution potential. A randomly selected TLM nanocrystal loaded tablet, was dispersed in 10 mL of distilled water by vortex mixing (30 s) with subsequent incubation for 30 min at 25 °C. The sample was analyzed for deviation in particle size, PI, ζ values and saturation solubility. The study was repeated in triplicates and their average values were documented [44,45].

2.2.7.2.4. Percentage drug content. The percentage drug content for tablets containing TLM nanocrystal was calculated by addition of a randomly selected tablet in volumetric flask containing 100 mL methanol. The sample was centrifuged (5000 rpm, 10 min) and the supernatant was subjected to the estimation of drug contents against blank using a double beam UV spectrophotometer. The study was repeated in triplicates and the results were documented [46,47].

2.2.7.2.5. In vitro drug release. The dissolution studies of the optimized batch of TLM nanocrystals loaded tablets were conducted to estimate drug release patterns of TLM in 900 mL of 0.1 M HCl. For comparison purpose, marketed tablets (Sartel® 20) as well as conventional tablets containing drug particles were also tested for dissolution. All other test parameters were kept as mentioned earlier in Section 2.2.5.4. Further, dissolution profiles of the optimized batch of TLM nanocrystals loaded tablets were also carried out in each of 900 mL of pH 6.8 phosphate buffer, pH 7.4 phosphate buffer and water, in order to estimate the effect of physiological pH on dissolution behavior of the final formulations [35,42]. The study was repeated in triplicates in order to confirm reproducibility of the results. Parameters like DE, MDT, f_1 and f_2 were calculated for comparison purpose [30–33].

2.2.7.2.6. Stability study. The stability study of the optimized batch of TLM nanocrystals loaded tablets, (n = 6) was carried out by charging the samples to HDPE bottles with 2 g desiccant for a period of 6 months at accelerated stability conditions (40 ± 2 °C/75% ± 5%RH). For estimation of physical stability, TLM nanocrystals loaded tablets were evaluated for variation in physical appearance, particle size, saturation solubility, hardness and drug content at predetermined time intervals [48,49].

2.2.7.2.7. In vivo pharmacokinetic study. Male Wister rats with an average weight of 200 ± 20 g and age ~10 weeks (on the day of study) were probed to estimate pharmacokinetic behavior of TLM nanocrystals loaded tablets against marketed tablets (Sartel® 20) as reference. The study was approved by the Institutional Ethics Committee of Department of Pharmaceutical Sciences, Saurashtra University, Rajkot, Gujarat, India (CPCSEA No: SU/DPS/IAEC/1003, Dated: 11/02/2010) and their guidelines were followed throughout the study. All the rats were acclimatized at a temperature of 20 ± 2 °C and relative humidity of 45 ± 15%, with a 12 h light/dark cycle over a period of 5 days. The animals were carefully observed to ensure their good health and suitability for inclusion in the study. For all rats, a standard laboratory diet (Pranav Agromart Ltd, Baroda, India) and domestic main tap water was available ad libitum. The animals were disconnected from diet at least 12 h before dosing. During study periods, rats were housed singly in polypropylene and stainless steel cages [14,15]. Twenty four rats were randomly divided into two groups (n = 12). Each rat of group I and group II was treated with the test and reference formulation, respectively. Samples for group I were prepared by dispersing TLM nanocrystals loaded tablets as test and samples of group II were prepared by dispersing marketed tablets as reference individually, in 2 mL of distilled water. All these samples were administered as oral formulations at a dose of 1.8 mg/kg [50] as a single dose by curved gastric gavage tubes directly into the stomach. The dose volume for all administration was maintained at 5 mL/kg [14,15]. Serial blood samples (500 μL) were collected from retro-orbital venous plexus with hematocrit over a period of 120 h. Rats of each group were further divided into two subgroups (n = 6) for convenient blood sampling over the entire study periods as recommended by the experts of IAEC (Institutional Animal Ethics Committee). Blood samples from each group were collected at predetermined time intervals, alternatively from each subgroup into heparinized plastic tubes. All these samples of whole blood were kept in refrigerated conditions (2–8 °C) until separation of plasma. Each sample was processed further by the in house developed bioanalytical method and subjected to HPLC analysis for the estimation of drug content [14,15]. The pharmacokinetic calculations were performed on the basis of plasma concentration–time data using Kinetica® version 5.1 (Thermo Scientific, USA) pharmacokinetics and pharmacodynamics software. Parameters like maximum plasma concentration (C_{max}), time to reach maximum concentration (t_{max}), area under the plasma concentration–time curve ($AUC_{0-\infty}$), area under the first moment curve ($AUMC_{0-\infty}$), terminal half-life ($t_{1/2}$), mean residence time (MRT), clearance (Cl) and half value duration (HVD). The relative bioavailability was calculated as the ratio of the mean oral $AUC_{0-\infty}$ of test formulation to that of reference formulation [51–55].

3. Results and discussions

3.1. Formulation and development of drug loaded nanosuspensions

Media milling offers distinctive advantages over other preparation methods of nanosuspensions which includes ease of scale-up, narrow size distribution, minimum batch-to-batch variation and flexibility for large scale. Moreover, during the reduction in particle size, no organic solvent is required and, it is hence an environmentally and economically

beneficial technology [56]. The energy input is delivered by high energy shear forces generated as a result of impaction of milling media with drug [57]. Further, this technique is most suitable with respect to least drug amorphization. This could be attributed to the ability of water to act as plasticizer on the surfaces of particles generated and thus lowering glass transition temperature (T_g) [9]. In light of these, media milling technique was employed as a simple, economic and efficient strategy for preparing drug loaded nanosuspensions.

3.2. Preliminary optimization of formulation parameters

In order to acquire the optimum composition of drug loaded nanosuspensions, the relationship between all possible variables should be thoroughly studied as follows [58].

3.2.1. Type of milling agents

The outcomes of optimization of type of milling agents for TLM loaded nanosuspensions revealed lower particle size and PI with zirconium beads compared to the same sized glass beads. This might be attributed to the harder and tougher nature of zirconium beads compared to that of equal sized glass beads. Hence, 1.0 mm sized zirconium beads were exploited as milling agents for all further trials of TLM loaded nanosuspensions [58].

3.2.2. Type of stabilizers

In the present investigation commonly exploited pharmaceutical polymers such as hydroxypropylcellulose (HPC), hydroxypropyl methylcellulose (HPMC E3), polyvinyl alcohol (PVA) and polyvinyl pyrrolidine (PVP K30) as well as nonionic surfactants like poloxamer 188, poloxamer 407 and tween 80 were explored as stearic stabilizers whereas an anionic surfactant such as sodium lauryl sulfate (SLS) was chosen as electrostatic stabilizer [59,60]. The results of particle size, PI and ζ illustrated that polymers were less effective than surfactants in terms of their ability to reduce particle size of drug particles. This could be attributed to the more effective wetting of drug particles by surfactants as compared to the polymers studied. The ζ values for the systems composed with stearic stabilizers were found in between −10 to −36 mV whereas for electrostatic stabilizer (SLS) it was on a higher side (>45 mV). The lower ζ values of stearic stabilizer might be due to their adsorbed layers of large molecules which shifts the shear plane to a longer distance from the particles [58,59]. Among all stabilizers studied, poloxamer 188 proved to be most efficient in terms of its ability to reduce particle size along with narrow particle size distribution. This could be attributed to the semicrystalline nature of poloxamers which strongly absorb onto the surface of hydrophobic drugs via their hydrophobic POP center block and POE chains [61,62]. As a consequence of this amphiphilic nature, nonionic surfactants became absorbed on to the surface of drug particles through an anchor segment and provide more effective particle size reduction [63]. Further, nanosuspensions were constructed with a combination of stearic (poloxamer 188) and electrostatic (SLS) stabilizers at a ratio of 1:1. There was a nonsignificant difference in particle size and PI values of drug loaded nanosuspensions as compared to the formulations constructed with stearic stabilizer (poloxamer 188) alone. However, ζ values of nanosuspensions constructed with combined stabilizers were on the higher side (>−38 mV). This might be attributed to the electronegativity provided by ionic stabilizer (SLS). It is worth mentioning that use of ionic stabilizers has been restricted due to their gastric irritation potential, higher sensitivity to pH change and destabilization of formulations in electrolyte rich environment [27]. Moreover, according to the literature, the ζ value of a stable colloidal systems should be more than |30 mV| [9,32]. This prerequisite was successfully achieved by using poloxamer 188 as a single stabilizer (−36.10 ± 1.43 mV). Therefore, the present investigation was persisted with poloxamer 188 as the single stabilizer.

3.2.3. Effect of concentration of drug

There was a substantial reduction in particle size when drug loading was reduced from 10% w/v to 5% w/v. However, there were no marked differences in particle size of systems with subsequent reduction in drug loading (2.5% w/v). These might be attributed to the reduction in total volume of material for size reduction with reduction in drug load. On the basis of significant reduction in particle size along with maximum possible drug load, 5% w/v of drug load was selected as optimum for all further trials [31,37].

3.2.4. Size of milling agents

The results demonstrated marked reduction in particle size values with small sized zirconium beads (0.5 mm). This might be accredited to an exponential increase in number of contact points between drug particles and milling agents at lower sized milling agents. However, there was nonsignificant decrease in particle size of TLM loaded nanosuspensions with further reduction in size of milling agents (0.2 mm). Moreover, it was easier to separate 0.5 mm and 1.0 mm sized beads from the product as compared to that of 0.2 mm [27,31]. Hence, 0.5 mm sized zirconium beads were selected as optimized milling agents for all further trials.

3.2.5. Time of stirring

The particle size decreased prominently up to a milling time of 16 h with subsequent cessation in the rate of reduction. This might be attributed to the fact that the majority of deagglomeration of drug particles had taken place initially and there was a consequent breakage of particles due to cleavage and fracture. The later process usually requires more mechanical stress [31]. In addition, lower rate of size reduction at higher milling time could also be explained by higher amount of stabilizer required to cover the freshly prepared surfaces of nanoparticles than that for the microparticles [27]. In comparison, among all time points, samples with 20 h stirring time had lowest values of particle size and PI and hence it was selected as optimum milling time for all further trials. Milling for the next 4 h led to an increase in particle size which might be attributed to an agglomeration due to the enhancement in kinetic energy with an additional input of energy. Hence, for all further trials 20 h was optimized as stirring time.

3.2.6. Stirring speed

The outcomes of stirring speed optimization illustrated a decrease in particle size with an intermediate stirring speed (750 rpm). The reduction in particle size could be justified by the generation of high energy and shear forces which provides enhanced impaction of milling agents and drug particles inside a milling chamber. However, there was a nonsignificant difference in particle size for batches prepared with 1000 rpm stirring speed compared to that of 750 rpm [22]. Hence, 750 rpm stirring speed was selected for all further trials of TLM loaded nanosuspensions.

3.2.7. Amount of milling agents

The results illustrated a minor difference in particle size and PI values for TLM loaded nanosuspensions when the amount of zirconium beads was varied from 1 to 5 g (20–100% w/v). Moreover, with higher amount of milling agents, [7.5 g (150% w/v)] there was a significant increase in particle size and PI values. This might be attributed to overfilling of milling chamber which ultimately results in unavailability of free space required for the collisions between drug particles and milling agents [22].

3.2.8. Drug to stabilizer ratio

Stabilizer concentration plays a vital role in the stability of nanosuspensions by contributing their absorption affinity on the surfaces of drug particles [63]. In the present study, drug to stabilizer ratios were varied from 1:1 to 20:1. The results suggested that particle size and PI values of TLM loaded nanosuspensions were increased at both higher and lower levels of stabilizer. This might be attributed

to an increase in viscosity of the systems at higher concentrations of stabilizer which hinders the formation of nanosuspension due to an additional obstruction [64]. Similarly, the increase in particle size and PI values at lower stabilizer concentrations might be attributed to insufficient amount of stabilizers present in the systems that could prevent agglomeration of drug particles (Ostwald ripening). The results depicted lowest values of particle size and PI in between 5:1 and 10:1 drug to stabilizer ratio.

3.3. Experimental design

On the basis of preliminary trials, concentration of stabilizer and amount of milling agents were identified as critical factors. Thus, the present study was conducted as a 3^2 full factorial design for TLM loaded nanosuspensions followed by PCA in order to scrutinize critical responses among all parameters studied, with the two factor concentration of stabilizer (X_1) and amount of milling agents (X_2) at five levels each [65]. The actual values of each of the selected factors have been summarized against their respective coded values in Table 1. The results of responses like particle size, saturation solubility (SS), polydispersibility index (PI) and zeta potential (ζ) for experimental design batches of TLM loaded nanosuspensions have been summarized in Table 2. The loading plot [Fig. 1(a)] depicts that PC1 was responsible for 80% of the total variance in the data set and PC2 was responsible for a further 20%. The results of all 9 batches were further treated with agglomerative hierarchy cluster analysis (AHCA) and its graphical display is shown in Fig. 1(b) as dendrogram. The results of dendrogram demonstrated clustering of the formulations into three major groups; group I (F1 and F9), group II (F5 and F6) and group III (F2, F3, F4, F7 and F8). Further, all the five groups were found to be relatively distant and substantially different from one another. Clusters of all formulations were correlated by PCA score plot in a similar way [Fig. 1(c)]. Correlation loading plot was constructed to decide most important variables for further optimization. The results scrutinized particle size and saturation solubility as two critical responses [Fig. 1(d)]. Further, both of these responses were plotted on the opposite sides of PC1 which suggested negative correlation between them. This result implies that if the particle size of nanosuspension is decreased, the saturation solubility would increase. Moreover, all other variables were plotted on correlation loading plot near to the origin and hence, they were not discussed. As displayed in 3D plots [Fig. 1(e, f)], the third principal component (PC3), had no additional variation in the data, against PC1 and PC2 and hence it was not considered for further studies. The scree plot for TLM loaded nanosuspensions [Fig. 1(g)] illustrates that the eigenvalues for each component were in descending order. The plot analysis depicted that the rate of decline tends to be fast first and then levels off with one large gap/break in the data between components 1 and 2 which indicated significance of the first two components (PC1 and PC2). All other components (PC3 and PC4) which appeared after the break were assumed to be trivial and hence removed from the study. This separation was further supported by the calculation of %CV for all components. The data for %CV of PC3 and PC4 accounts for almost 100% variation which justified removal of these terms [12,13]. At the end, it was speculated that the particle size and saturation solubility were the most important variables in the preparation of TLM loaded nanosuspensions and hence, they were further selected for the study. For all 9 batches, both dependent variable particle size (Y_1) and saturation solubility (Y_2) exhibited wide variations from 330.33 to 470.67 nm and 1211.23 to 4438.26 μg/mL, respectively (Table 2). The data clearly indicate strong influence of the selected factors (X_1 and X_2) on responses (Y_1 and Y_2) [26]. A stepwise multivariate linear regression was performed to evaluate the observations.

For particle size (Y_1), and b_{12} whereas for saturation solubility (Y_2), coefficients b_{22} and b_{12}, were found to be insignificant ($P > 0.05$) and hence, these terms were separated from their respective full model in order to develop a reduced model. The removal of insignificant terms was further justified by executing an ANOVA test (Table 3). The high values of correlation coefficients for particle size (Y_1) and saturation solubility (Y_2) illustrate goodness of fit. The critical values of F for Y_1 and Y_2 were found to be 10.13 ($df = 1, 3$) and 9.55 ($df = 2, 3$), respectively. For both responses, calculated F values [0.91 (X_1), 0.80 (X_2)] were less than their respective critical values which suggested nonsignificant differences among the full and reduced model [22,23].

3.3.1. Influence of formulation composition factor on particle size (Y_1)

The results of regression analysis for particle size (Y_1) depicted negative sign for regression coefficients b_1 and b_2 which suggested that with an increase in concentration of stabilizer and amount of milling agents, particle size of TLM loaded nanosuspensions decreases. A lowest particle size of 330.33 nm was observed with Batch TLM-NS-F6. However, the results of response surface, contour and perturbation plots illustrated an increase in particle size of drug loaded nanosuspensions at both high and low concentrations of stabilizer. This could be justified by an increase in viscosity of the systems at higher stabilizer concentration which hinders the processing of nanosuspension [27,28]. Insufficient amount of stabilizers with lower ability to prevent agglomeration of drug particles (Ostwald ripening) might be the reason for an increase in particle size at lower stabilizer concentrations. Further, lowest particle size at higher amount of milling agents could be justified by the increase in probability of collisions between milling agents and drug particles inside a milling chamber [31].

3.3.2. Influence of formulation composition factor on saturation solubility (Y_2)

The results of regression analysis for saturation solubility (Y_2) depicted positive sign for regression coefficients b_1 and b_2 which suggested that with an increase in concentration of stabilizer and amount of milling agent saturation solubility of TLM loaded nanosuspensions also increases. Batch TLM-NS-F6 exhibited the highest saturation solubility of 4438.26 μg/mL among all experimental design batches. However, the results of response surface, contour and perturbation plots exemplified a decrease in saturation solubility at both high and low concentration of stabilizers. This could be explained by a relative increase in their particle size. Similarly, highest saturation solubility of systems at

Table 2
Responses of 3^2 full factorial design batches of TLM loaded nanosuspensions.

Batch code	Particle size (nm)	Saturation solubility (μg/mL)	Polydispersibility index	Zeta potential (mV)
TLM-NS-F1	470.67 ± 10.60	1211.23 ± 54.73	0.18 ± 0.07	−27.55 ± 2.67
TLM-NS-F2	423.67 ± 8.43	2190.14 ± 76.56	0.18 ± 0.03	−29.90 ± 3.78
TLM-NS-F3	406.00 ± 4.65	2837.47 ± 98.54	0.13 ± 0.04	−31.55 ± 5.61
TLM-NS-F4	390.33 ± 6.87	3056.09 ± 101.66	0.18 ± 0.03	−32.73 ± 3.67
TLM-NS-F5	356.67 ± 8.40	4431.10 ± 114.70	0.10 ± 0.07	−34.85 ± 6.52
TLM-NS-F6	330.33 ± 6.88	4438.26 ± 109.78	0.12 ± 0.02	−35.76 ± 1.55
TLM-NS-F7	424.00 ± 5.32	2630.13 ± 71.00	0.16 ± 0.02	−30.63 ± 3.70
TLM-NS-F8	386.00 ± 8.43	3073.91 ± 96.12	0.15 ± 0.04	−32.46 ± 6.54
TLM-NS-F9	367.33 ± 9.11	3876.25 ± 89.80	0.14 ± 0.02	−32.10 ± 1.43

The results are mean ± SD (n = 3).

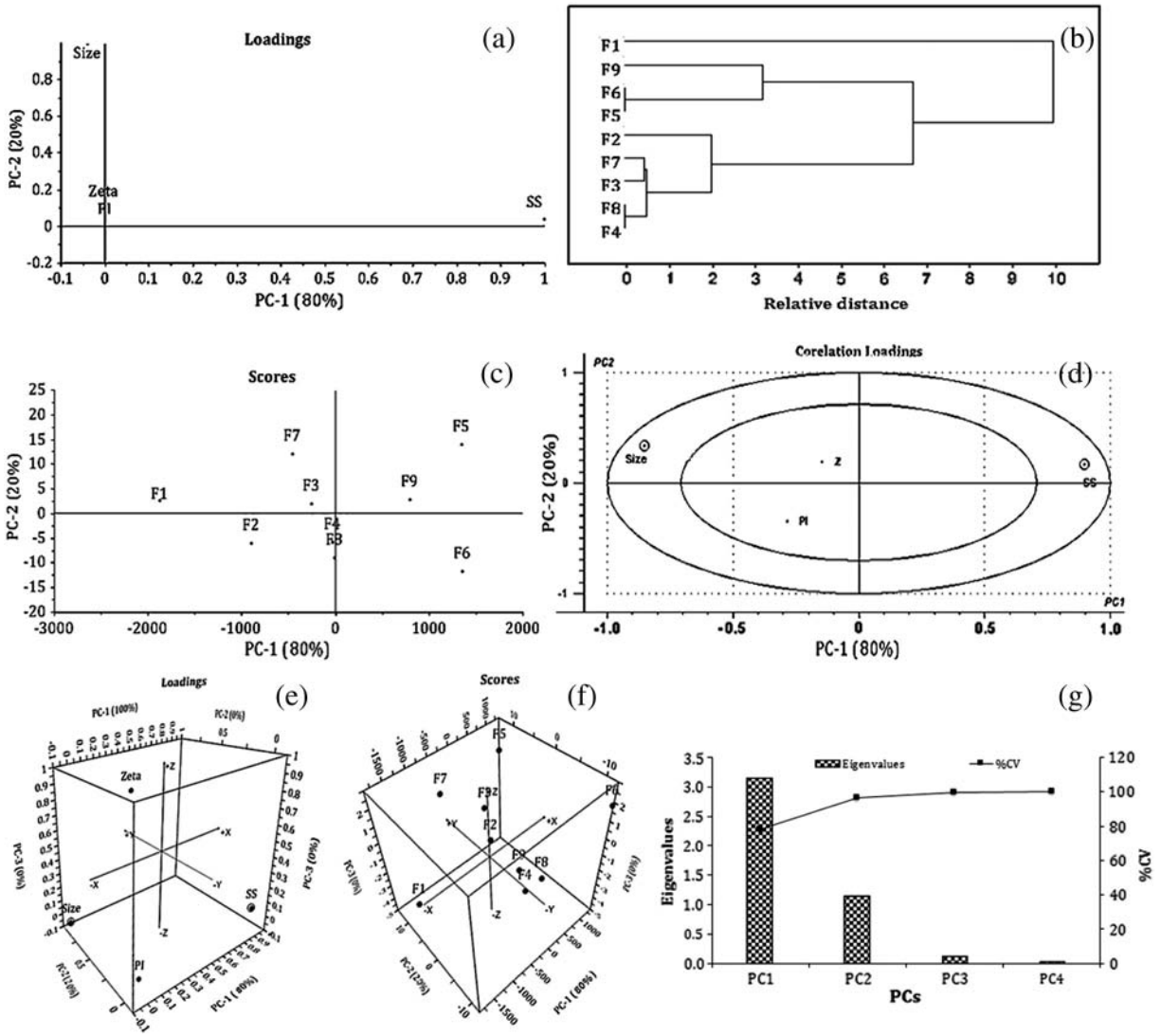

Fig. 1. PCA study for TLM loaded nanosuspensions (a) loading plot, (b) dendrogram, (c) score plot, (d) correlation loading plot, (e) 3-D loading plot, (f) 3-D score plot and (g) scree plot.

Table 3
Summary of ANOVA study for TLM loaded nanosuspensions.

Particle size (Y_1)				
	DF[a]	*SSR*[b]	*MS*[c]	$R^2 = 0.9962$ Fcal = 0.91
Regression				Fcritical = 10.13 DF = (1, 3)
FM[d]	5	13,965.58	2793.12	
RM[e]	4	13,953.33	3488.33	
Residual				
FM	3	40.42	13.47	
RM	4	52.67	13.17	
Saturation solubility (Y_2)				
	DF	*SSR*	*MS*	$R^2 = 0.9560$ Fcal = 0.80
Regression				Fcritical = 9.55 DF = (2, 3)
FM	5	8,597,271	1,719,454	
RM	3	8,461,416	2,820,472	
Residual				
FM	3	253,091.1	84363.7	
RM	5	388,946.7	77,789.33	

[a] DF: Degree of freedom.
[b] SSR: Sum of square residuals.
[c] MS: Mean of squares.
[d] FM: Full model.
[e] RM: Reduced model.

higher amount of milling agents could be attributed to an increase in collisions between milling agents and drug particles inside a milling chamber [27,28].

3.3.3. Model validation and check point batch analysis

Criteria for the optimized batch were arbitrarily selected as minimum particle size and maximum saturation solubility. Check point/optimized batch of TLM loaded nanosuspensions was prepared practically with concentration of stabilizer (X_1) as 0.79% w/v and amount of milling agent (X_2) as 4.26 g. The results depicted nonsignificant ($P > 0.05$) difference and lower % relative error between experimentally obtained and theoretically computed data of particle size and saturation solubility which suggested suitability of the design applied (Table 4).

3.4. Evaluation parameters of drug loaded nanosuspensions

3.4.1. Particle size and size distribution

Particle size and size distribution are the key parameters for evaluating the physical stability of nanosuspensions [16]. The continual dissolution of the small particles and recrystallization of solute on the surface of large particles results into Ostwald ripening [64]. The particle size of the optimized batch of TLM loaded nanosuspension was found to

Table 4
Summary and results of optimized batch of TLM loaded nanosuspensions.

Type of component		Name of component	Optimized levels
Concentration of stabilizer (X_1)		Poloxamer 188	0.79% w/v
Amount of milling agent (X_2)		Zirconium beads	4.26 g
Responses	Predicted value	Experimental value[a]	% relative error
Particle size (nm)	332.08	334.67 ± 10.43	0.65
Saturation solubility (μg/mL)	4814.11	4778.42 ± 111.98	0.74

[a] The results are of mean ± SD (n = 3).

be 334.67 nm which confirmed the nanometer size of the developed formulation (Fig. 2). The results depicted a narrow size distribution for the optimized batch of TLM loaded nanosuspensions (PI value — 0.12), as compared to its coarse suspensions (PI value 0.87) with wider distribution. The narrow size distribution of TLM loaded nanosuspensions supports the absence of Ostwald ripening by eliminating different solute concentrations among the medium [20].

3.4.2. Saturation solubility

Independent of any of administration routes, drug solubility is an essential factor for its effectiveness. The enhanced saturation solubility of drug provides an accomplishment of targeted therapeutic goals with much smaller dosage [37]. The optimized batch of TLM loaded nanosuspension had a saturation solubility of 4778.42 μg/mL compared to 256.34 μg/mL for its coarse suspensions which illustrated poor water solubility of TLM.

3.4.3. Zeta potential (ζ)

Zeta potential (ζ) is an electric potential of the shear plane attached to the moving particles in the medium and it is generally utilized for the prediction of stability of nanosuspensions [9,10]. The decrease in ζ value with decrease in concentration of stabilizer may be attributed to the inability of stabilizer to prevent particle agglomeration at lower concentrations. The results of the optimized batches of TLM loaded nanosuspension depicted the ζ values of more than |30 mV|, which suggested physical stability formulations developed [9].

3.4.4. In vitro drug release

All batches of experimental design exemplified significant enhancement in the dissolution rate as compared to its coarse drug suspension. The dissolution pattern of the optimized batch of TLM loaded nanosuspension showed 69.42% of drug release within 15 min, compared to only 7.45% for TLM loaded coarse suspension (Fig. 3). The significantly higher ($P < 0.05$) values of $\%DE_{10\ min}$ and lower values of MDT for the optimized batch of TLM loaded nanosuspension as compared to its coarse drug suspensions suggested marked improvement in dissolution rate of TLM by the developed nano sized formulations [27,28]. Moreover, parameters like f_1 and f_2 confirmed nonsimilarity of dissolution profiles of TLM loaded nanosuspension and its coarse drug suspensions as f_1 was higher than 15 and f_2 was lower than 50 [30–34]. The increase in dissolution velocity of TLM loaded nanosuspension could be attributed to reduction in particle size, increase in surface area and decrease in diffusion distance [57–59].

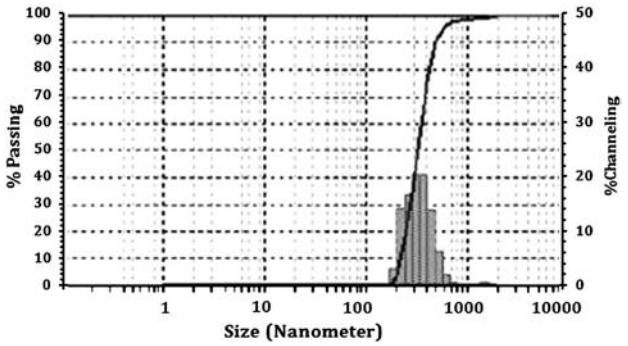

Fig. 2. Particle size analysis graph for optimized batches TLM loaded nanosuspensions.

3.4.5. Transmission electron microscopy (TEM)

The morphology of drug particles in nanosuspensions depended on the stabilizer used and amount of drug loaded [49]. Morphological and structural examination of the optimized batches of TLM loaded nanosuspension using transmission electron microscope illustrated a formation of sphere shape drug nanoparticles (Fig. 4). The nanoparticle size observed by TEM was in good agreement with that of PCS [49,50].

3.4.6. Short term physical stability

Short term physical stability of optimized batches of TLM loaded nanosuspension was evaluated at 25 °C since it was supposed to be converted into a solid intermediate (drug nanocrystals) by a process of lyophilization [57]. The results illustrated nonsignificant alteration in all measured parameters of TLM nanocrystals over a period of 7 days. This might be attributed to the stearic hindrances provided by steric stabilizer (Poloxamer 188) against the aggregation of nanocrystals [27,28].

3.5. Formulation and development of drug nanocrystals

3.5.1. Preparation of drug nanocrystals by lyophilization

Lyophilization process was selected in the present investigation for drying of the optimized batch of TLM loaded nanosuspension ahead of spray drying. This might be attributed to higher temperature application for spray drying [39]. Moreover, lyophilization is a well-established pharmaceutical unit operation for developing pharmaceutical powders with improved solubility properties especially from aqueous solutions [40]. The present study involved screening of four different cryoprotectants at four concentrations each in order to protect nanoparticles from various

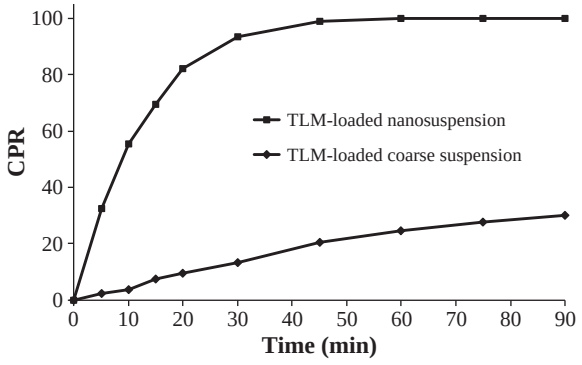

Fig. 3. Comparison of in vitro drug release profiles of the optimized batch of TLM loaded nanosuspension against its respective coarse suspensions in 0.1 M HCl, error bar represents SD (n = 3).

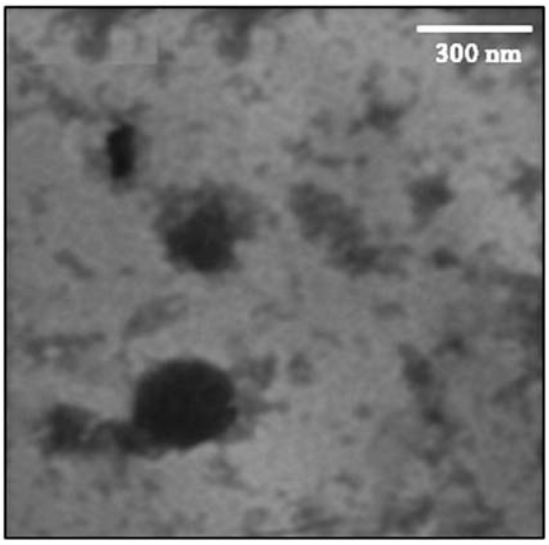

Fig. 4. TEM photograph of optimized batch of TLM loaded nanosuspension.

stresses generated during the process. Usually, a higher concentration of cryoprotectant and a faster freezing rate results in an enhanced redispersibility of nanoparticles [55,56]. Three essential features of lyophilized product namely; color, appearance and ease of redispersibility (redispersion time), were selected in order to evaluate the effect of cryoprotectants by using a scoring method [33,36]. All three criteria had a range of values from 0 to 10, with higher scores indicating better properties. The surface collapse and particle agglomeration were visually observed in glucose and sucrose based formulations. This might be related to the capillary pressure theory which explains that agglomeration occurs as a result of the capillary forces encountered during the drying operation. The data illustrated highest scoring values with 5% w/v of trehalose for TLM loaded samples. Moreover, the optimal lyophilized batch of TLM nanocrystal was readily redispersed into homogeneous nanosuspensions within 30 s which signified ease of dispersibility of TLM nanocrystals.

3.5.2. Solid state characterization of lyophilized drug nanocrystals

3.5.2.1. Fourier transform infra-red spectroscopy (FT-IR). FT-IR study was conducted to characterize any possible interaction between drug and excipients utilized. On comparing the spectra of drug powder with the optimized batch of lyophilized drug nanocrystals, there was no remarkable difference of characteristic peaks in terms of peak position and trend. The identical FT-IR spectra curves proposed the unchanged molecular structure of TLM even after the process of wet milling and lyophilization. The broadening of peaks was observed with TLM nanocrystals which might be caused by surface adsorption of stabilizers [38–40].

Table 5
Effect of lyophilization on particle size, PI, zeta potential and saturation solubility of optimized formulations.

Parameters	Nanocrystals	Nanosuspension
Particle size (nm)	336.67 ± 12.44	334.67 ± 10.43
PI	0.15 ± 0.03	0.12 ± 0.02
Zeta Potential (mV)	−33.56 ± 1.51	−35.35 ± 1.25
Saturation solubility (μg/mL)	4667.42 ± 105.03	4778.42 ± 111.98

The results are of mean ± SD (n = 3). PI: Polydispersibility Index.

3.5.2.2. Differential scanning calorimetry (DSC). Generation of amorphous regions in crystalline nanoparticles is undesirable due to high reactivity of amorphous phase. The analysis of the optimized batch of TLM nanocrystals by DSC illustrated retention of drug crystallinity after milling and lyophilization. The endothermic peak (262.74 °C) of TLM nanocrystals was not as sharp as its drug powder (262.98 °C) which indicated a minor loss of drug crystallinity. Moreover, the lyophilized batch of TLM nanocrystals showed an additional peak near 55 °C which was indicative of the presence of Poloxamer 188 [38–40]. This could be explained by the presence of water during wet milling which might have a considerable impact on the solid state transformation of drug molecules by acting as plasticizer [37].

3.5.2.3. Powder X-ray diffraction (PXRD). The effect of wet milling and lyophilization on the drug crystallinity of the optimized batch of TLM nanocrystals against its drug powder have been studied by PXRD study. The results showed distinct peaks at 5.54°, 10.22°, 11.82°, 14.18°, 17.24°, 22.16° and 27.48° for TLM sample which suggested highly crystalline nature TLM. Further, the results depicted more prominent peaks near to the base line (at 2θ of 18° and 23°) for TLM nanocrystals which might be attributed to the presence of Poloxamer as stabilizer [19,20]. On the contrary, XRD pattern of drug nanocrystals illustrated most of the peaks at the same position as those of original drug, along with varying intensities. This difference could be attributed to the application of high shear during wet milling, the presence of cryoprotectant (trehalose) and the presence of Poloxamer 188 at the surface of the

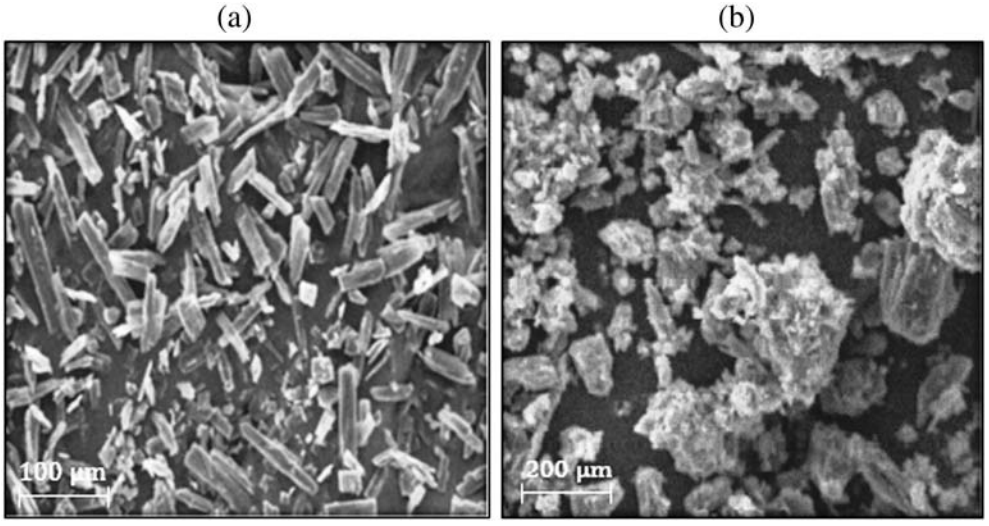

Fig. 5. SEM photographs of (a) TLM and (b) optimized batch of lyophilized TLM nanocrystals.

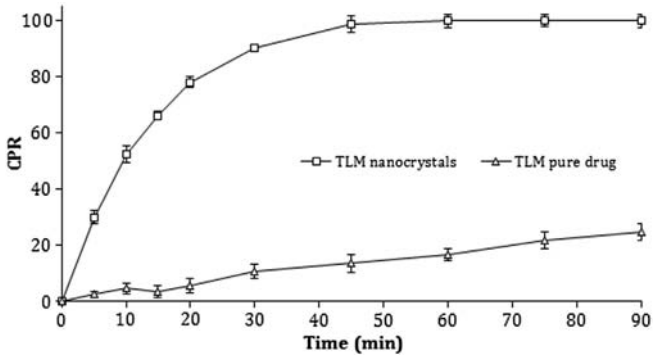

Fig. 6. Comparison of in vitro dissolution profiles of optimized batch of TLM nanocrystals against drug particles in 0.1 M HCl, error bar represents SD (n = 3).

nanoparticles [38–40]. However, specific drug peaks were preserved in their respective lyophilized samples of TLM nanocrystals without significant change in the intensity, which illustrated that the drug crystallinity of the sample was conserved even after the process of wet milling and lyophilization. It is well-known that amorphous substances are associated with higher solubility than crystalline ones whereas crystalline substances are physically more stable [9]. These results confirmed that the process of wet milling and lyophilization does not influenced the crystalline state of TLM significantly.

3.5.2.4. Scanning electron microscopy (SEM). SEM images of drug powder and optimized batch of lyophilized TLM nanocrystals illustrated significant difference in drug particles, not only in size but also in shape (Fig. 5) [20]. The drug powder sample exhibited lack of particle size uniformity and its size was larger than its sample of drug nanocrystals. On the contrary, the milled nanocrystals exhibited uniformity in particle size and absence of larger particles. SEM micrograph of drug powder revealed large crystalline blocks whereas the optimized batch of TLM nanocrystals was found to be rod-shaped without sharp edges. The drug nanocrystals appeared to be agglomerated owing to the presence of stabilizer on the surface [42,43].

3.5.3. Evaluation parameters for lyophilized drug nanocrystals

3.5.3.1. Particle size and size distribution. After reconstituting the optimized batch of lyophilized TLM nanocrystals, there was a nonsignificant alteration in particle size as well as PI in comparison to that of the optimized batch of TLM loaded nanosuspensions (Table 5). This might be attributed to the aggregation prevention properties of cryoprotectants (trehalose) in addition to stabilizer (Poloxamer 188) [43].

Table 6
Reconstitution potential of drug nanocrystals loaded tablets with respect to drug loaded nanosuspensions.

Parameters	Nanocrystals containing tablets	Nanosuspension
Particle size (nm)	341.00 ± 11.65	334.67 ± 10.43
PI	0.14 ± 0.05	0.12 ± 0.02
Zeta potential (mV)	−32.43 ± 0.24	−35.35 ± 1.25
Saturation solubility (μg/mL)	4415.6 ± 121.78	4778.42 ± 111.98

The results are mean ± SD (n = 3). PI: Polydispersibility Index.

3.5.3.2. Saturation solubility. The optimized batch of lyophilized TLM nanocrystals exhibited nonsignificant differences in saturation solubility with respect to that of the optimized batch of TLM loaded nanosuspension (Table 5) which depicted suitability of the lyophilization method [30].

3.5.3.3. Zeta potential (ζ). The results suggested nonsignificant ($P < 0.05$) decrease in ζ value for the optimized batch of reconstituted TLM nanocrystals as compared to freshly prepared optimized batch of TLM loaded nanosuspension. Nonetheless, the values obtained before and after lyophilization were higher than |30 mV|, which supported physical stability of the system (Table 5) [30].

3.5.3.4. Percentage drug content. For the optimized batch of lyophilized TLM nanocrystals, drug content was found to be 98.34% with low values of standard deviation. This indicated homogeneous drug distribution in the developed formulation and reproducibility of results [30].

3.5.3.5. In vitro drug release. TLM nanocrystals exemplified significant improvement in the dissolution rate as compared to its drug sample. The release profile of the optimized batch of TLM nanocrystals showed 82.54% of TLM release within 15 min in comparison to only 3.67% with TLM drug particles (Fig. 6). The significantly higher values of $\%DE_{10\ min}$ and lower values of MDT for the optimized batch of TLM nanocrystals as compared to its drug particles suggested marked improvement in dissolution rate by the developed nano sized formulations [10,11]. Moreover, parameters like f_1 and f_2 confirmed nonsimilarity of dissolution profiles of drug nanocrystals and its drug particles as the f_1 value was higher than 15 and the f_2 value was lower than 50 [30–34]. The increase in dissolution velocity of TLM nanocrystals could be attributed to the reduction in particle size, increase in surface area and decrease in diffusion distance whereas the incomplete drug release of drug particles could be attributed to the large crystal size [10].

3.5.3.6. Stability study. Reduction of particle size generally results in an increase in surface area of along with an increased free energy. Smaller particles tend to decrease this energy as a result of agglomeration caused by Ostwald ripening [32]. The physical stability data of

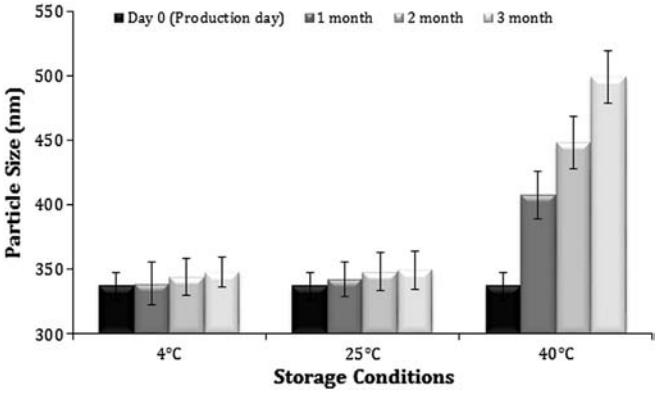

Fig. 7. Effect of storage condition on particle size of optimized batch of TLM nanocrystals, error bar represents SD (n = 3).

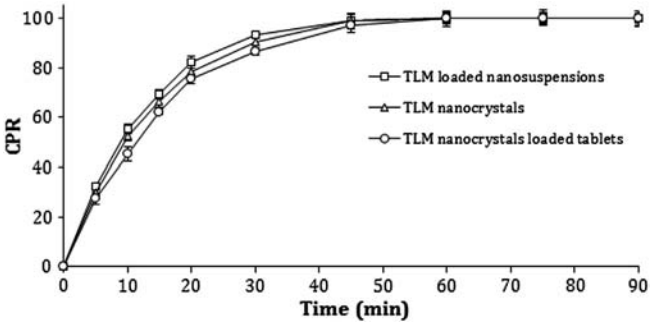

Fig. 8. Comparison of in vitro drug release profiles of TLM loaded nanosuspension, lyophilized drug nanocrystals and tablets comprising nanocrystals, error bar represents SD (n = 3).

lyophilized TLM nanocrystals are summarized in Fig. 7 which provides an overview of particle size, PI and zeta potential varied at different storage temperatures over a period of 6 months. The results depicted a non-significant increase in all parameters studied over the period of 6 months storage at 4 ± 2 °C and 25 ± 2 °C. However, for the samples stored at 40 ± 2 °C there was a remarkable increase in all three parameters studied. The potential long-term stability for the wet-milled lyophilized systems could be explained by long swinging hydrophilic EO chains of Poloxamer 188 on the particle surface that provide an excellent steric hindrance which prevents particles from aggregating [32]. Moreover, the homogeneous particles (low PI values) hinder the dissolution of smaller particles and growth of larger particles, i.e. Ostwald ripening.

3.5.4. Formulation and development of drug nanocrystals loaded tablets

3.5.4.1. Preparation of drug nanocrystals loaded tablets. With an aim of providing maximum patient compliance the optimized batch of TLM nanocrystals was transformed into tablets as the most compliable solid oral unit dosage forms. MCC PH 200 was used as directly compressible diluent owing to its better flowability compared with other grades of MCC as well as disintegration property [47].

3.5.4.2. Evaluation parameters of drug nanocrystals loaded tablets

3.5.4.2.1. Flowability of pre-compressed blends. The present study involved direct compression as a method for preparing drug nanocrystals loaded tablets and good flow property of the precompression blend was a prerequisite criterion. The results of flowability study of ready for compression (RFC) blends of batches of drug nanocrystals loaded tablets revealed excellent flowability [44].

3.5.4.2.2. Physical characterization. The results of all physical characterization tests revealed that all batches of prepared tablets complied with the required pharmacopoeial specifications [46]. The data for hardness analysis revealed higher values for TLM nanocrystals loaded tablets compared to conventional tablets. This might be attributed to the fact that compaction of smaller particles generally results in harder tablets due to an availability of increased area for binding. The lower values of % friability for TLM nanocrystals loaded tablets, indicated stronger interaction of nanoparticles with the filler (MCC) than that of respective drug particles [47].

3.5.4.2.3. Reconstitution potential. Drug nanocrystals loaded tablets should disperse quickly and completely when subjected to aqueous environment under mild agitation. The results of reconstitution potential of optimized batch TLM nanocrystals loaded tablets have been summarized in Table 6. The data illustrated nonsignificant difference between all the parameters evaluated as compared to its optimized batch of nanosuspension. This depicted the capability of the drug nanocrystals to remain in nanometer size irrespective of change in dosage form [47].

3.5.4.2.4. Percentage drug content. The values of drug content were almost 100%, along with very low standard deviations which suggested uniform dispersion of the drug in developed formulations. The value of % drug content for the batches of TLM nanocrystals loaded tablets was found to be 98.94.

3.5.4.2.5. In vitro drug release. As shown in Fig. 8, TLM nanocrystals loaded tablets had slightly lower rate of dissolution as compared to its optimized batch of nanosuspension and nanocrystals whereas there was no remarkable difference in the in vitro release profiles of optimized batch of TLM loaded nanosuspension and TLM nanocrystals. This might be attributed to the effect of the type of dosage form (compressed tablets). Lower values of $\%DE_{10\ min}$ and higher values of MDT for the optimized batch of TLM nanocrystals loaded tablets as compared to its nanocrystals and nanosuspension also recommended slightly lower rate of dissolution for tablet dosage form. In addition to this, a comparison between the dissolution profiles of TLM nanocrystals loaded tablets, TLM nanocrystals and TLM loaded nanosuspensions using f_1 and f_2 depicted nonsignificant differences between all of them as the value of f_1 was lower than 15 and the value of f_2 was higher than 50 [30–34]. The results of comparison of in vitro release profiles for the optimized batch of TLM nanocrystals loaded tablets, marketed formulations (Sartel® 20) and conventional tablets containing drug particles illustrated remarkable improvement in dissolution rate by nanocrystal loaded tablets as compared to the other two formulations (Fig. 9). The values of $\%DE_{10\ min}$ were highest for TLM nanocrystals loaded tablets followed by marketed tablets and conventional tablets. Similarly, the values of MDT followed the reverse pattern as conventional tablets > marketed tablets > drug nanocrystals loaded tablets. The dissimilarity between all these profiles was further confirmed by higher values of f_1 (>15) and lower values of f_2 (<50). Further, in vitro dissolution of TLM nanocrystals loaded tablets have been carried out in various dissolution media of different pH in order to prove the robustness of dissolution enhancement of the developed formulation (Fig. 10). The results suggested that TLM nanocrystals loaded tablets exhibited slightly higher rate of dissolution in 0.1 M HCl compared to the other three dissolution media (pH 6.8 phosphate buffer, water, pH 7.4 phosphate buffer). This might be attributed to the fact that TLM has a pH-dependent release pattern with highest solubility at acidic pH. However, there was a non-significant ($P < 0.05$) difference in the values of $\%DE_{10\ min}$ and MDT. This was further confirmed by the lower value of f_1 (<15) and higher value of f_2 (>50) [30–34].

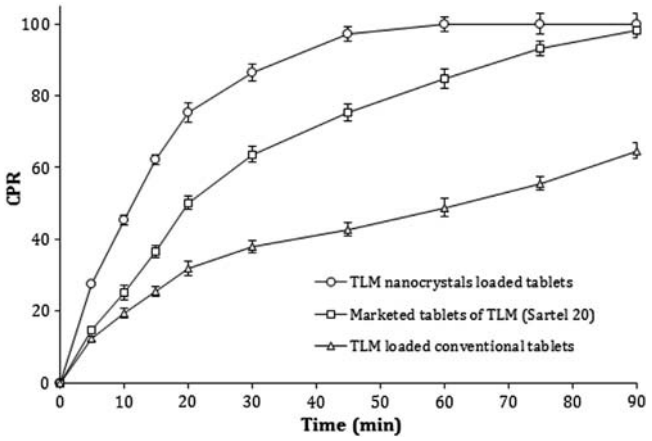

Fig. 9. Comparison of in vitro drug release profiles of TLM loaded tablets comprising nanocrystals, marketed tablets and conventional tablets in 0.1 M HCl, error bar represents SD (n = 3).

3.5.4.2.6. Stability study. A stability study of the TLM nanocrystals loaded tablets was carried out as per the ICH guidelines on accelerated stability conditions [40 ± 2 °C and 75 ± 5% RH for a period of 6 months]. The results illustrated nonsignificant ($P < 0.05$] change in physical appearance, particle size, saturation solubility, hardness, and % drug content of all formulations analyzed at predetermined time intervals compared to the samples which have been stored initially

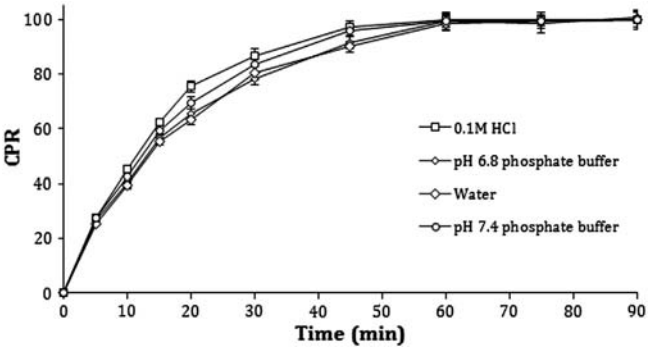

Fig. 10. Effect of pH of dissolution media on in vitro drug release profiles of tablets comprising TLM nanocrystals, error bar represents SD (n = 3).

Table 7
Accelerated stability study of optimized batches of drug nanocrystals loaded tablets.

Parameters	Storage periods			
	Day 0	1 month	3 months	6 months
Physical appearance	Off white	Off white	Off white	Off white
Particle size (nm)	341.00 ± 11.65	344.33 ± 15.16	347.67 ± 14.11	351.33 ± 15.15
Saturation solubility (μg/mL)	4415.6 ± 121.78	4353.67 ± 115.76	4213.65 ± 101.46	4111.5 ± 99.62
Hardness (kg/cm^2)	5.78 ± 1.06	5.66 ± 1.16	5.59 ± 0.92	5.47 ± 0.88
Drug content (%)	98.24 ± 0.13	100.04 ± 0.95	101.01 ± 1.01	98.02 ± 1.04

The results are mean ± SD (n = 3).

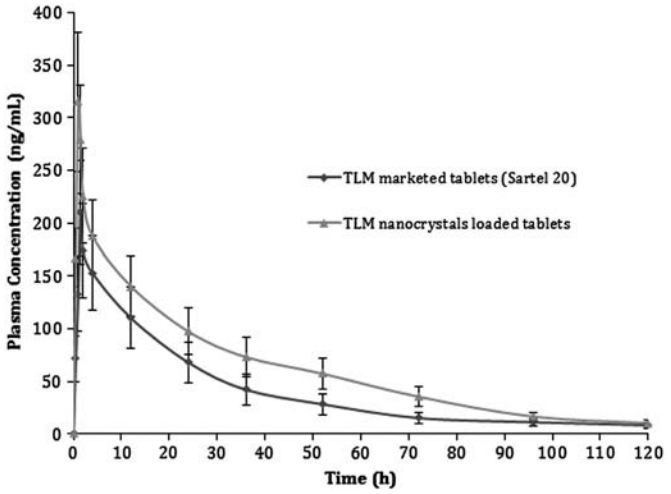

Fig. 11. Comparison of in vivo pharmacokinetic profiles of TLM nanocrystals loaded tablets against its marketed tablets, error bar represents SD (n = 6).

(Table 7). This proposed stability of the final dosage forms for at least 6 months under the accelerated storage conditions [42,43].

3.5.4.2.7. In vivo pharmacokinetic study. The plasma concentrations–time profiles of TLM nanocrystals loaded tablets and marketed tablets are shown in Fig. 11 along with their pharmacokinetic parameters (Table 8). The absorption profile of TLM nanocrystals loaded tablets was higher than that of marketed tablets at each time point which might be attributed to very low aqueous solubility and poor dissolution properties of TLM in its raw form. Compared with marketed tablets comprising drug particles, the developed drug nanocrystals loaded tablets were more effective to improve rate and extent of oral absorption of TLM. This could be explained by the potential of nanosuspensions to deliver drug molecules in nanometer size with a simultaneous increase in surface area for oral absorption. These findings were consistent with results from the dissolution study advocating that the differences in absorption were primarily attributed to the dissolution behavior of drug with different particle sizes [52–56].

Table 8
Results of in vivo pharmacokinetic study of drug nanocrystals loaded tablets and marketed tablets.

Parameters	Group I[a]	Group II[b]
C_{max} (ng/mL)	315.32 ± 63.16	210.4 ± 72.65
T_{max} (h)	1.36 ± 0.65	1.55 ± 0.19
$AUC_{0-\infty}$ (ng·h/mL)	7946.49 ± 883.26	5593.95 ± 845.66
$AUMC_{0-\infty}$ (ng·h^2/mL)	274471.76 ± 6256.57	203731.65 ± 4656.73
$t_{1/2}$ (h)	23.03 ± 1.03	23.88 ± 1.34
MRT (h)	34.54 ± 1.75	36.42 ± 2.68
Clearance (mL/h)	0.04530 ± 0.0032	0.06435 ± 0.0037
HVD (h)	8.31 ± 0.87	10.08 ± 0.56
$\%F_{Rel}$	149.86	–

The results are mean ± SD (n = 6).
[a] Test formulation: Drug nanocrystals loaded tablets by oral route.
[b] Reference formulation: Marketed tablet by oral route.

4. Conclusions

The results designated successful utilization of nanosuspension as a vehicle for oral drug delivery of a poorly water soluble drug, TLM. The in vitro and in vivo enhancement by the developed nanosized dosage forms is attributed to reduction in size of drug molecules and increase in effective surface area. Further, nanosuspension illustrated efficacious conversion of optimized formulations into most patient compliable solid oral dosage forms, i.e. tablets, which suggests productive amalgamation of novel drug delivery systems with the conventional dosage form. The developed formulations exhibited improvement in the results of in vitro and in vivo studies as compared to their respective marketed tablets (Sartel® 20). However, the developed formulation requires extensive clinical trials before commercialization for human use.

Acknowledgment

We would like to thank Torrent Research Center for providing gift sample of Telmisartan.

References

[1] C.A. Lipinski, Drug-like properties and the causes of poor solubility and poor permeability, J. Pharmacol. Toxicol. Methods 44 (2000) 235–249.
[2] K. Wening, J. Breitkreutz, Oral drug delivery in personalized medicine: unmet needs and novel approaches, Int. J. Pharm. 404 (2011) 1–9.
[3] H. Gupta, D. Bhandari, A. Sharma, Recent trends in oral drug delivery: a review, Recent Pat. Drug Deliv. Formul. 3 (2009) 162–173.
[4] L.M. Ruilope, Telmisartan for the management of patients at high cardiovascular risk, Curr. Med. Red. Opin. 27 (2011) 1673–1682.
[5] S.C. Sweetman, Martindale — The Complete Drug Reference, Pharmaceutical Press, London, 2005.
[6] S.N. Kothawade, N.R. Kadam, P.D. Aragade, D.G. Baheti, Formulation and characterization of telmisatan solid dispersions, Int. J. Pharm. Technol. Res. 2 (2010) 341–347.
[7] B. Patel, R.H. Parikh, D. Swarnakar, Enhancement of dissolution of telmisartan through the use of solid dispersion technique-surface solid dispersion, J. Pharm. Bioall. Sci. 4 (2012) 64–68.
[8] Y. Zhang, T. Jiang, Q. Zhang, S. Wang, Inclusion of telmisartan in mesocellular foam nanoparticles: drug loading and release property, Eur. J. Pharm. Biopharm. 76 (2010) 17–23.
[9] R.H. Müller, C. Jacobs, O. Kayser, Nanosuspensions as particulate drug formulations in therapy: rationale for development and what we can expect for the future, Adv. Drug Deliv. Rev. 47 (2001) 3–19.
[10] W. Libo, Z. Jian, W. Wiwik, Physical and chemical stability of drug nanoparticles, Adv. Drug Deliv. Rev. 63 (2011) 456–469.
[11] A.A. Date, V.B. Patravale, Current strategies for engineering drug nanoparticles, Curr. Opin. Colloid Interface Sci. 9 (2004) 222–235.
[12] G. Kaul, J. Huang, R. Chatlapalli, K. Ghosh, A. Nagi, Quality-by-design case study: investigation of the role of poloxamer in immediate-release tablets by experimental design and multivariate data analysis, AAPS PharmSciTech 12 (2011) 1064–1076.
[13] R.A. Lionberger, S.L. Lee, L. Lee, A. Raw, L.X. Yu, Quality-by-design: concepts for ANDAs, AAPS J. 10 (2008) 268–276.
[14] T. Niwa, S. Miura, K. Danjo, Universal wet-milling technique to prepare oral nanosuspension focused on discovery and preclinical animal studies — development of particle design method, Int. J. Pharm. 405 (2011) 218–227.
[15] P. Balakrishnan, B.J. Lee, D.H. Oh, J.O. Kim, M.J. Hong, J.P. Jee, J.A. Kim, B.K. Yoo, J.S. Woo, C.S. Yong, H.G. Choi, Enhanced oral bioavailability of dexibuprofen by a novel solid self-emulsifying drug delivery system (SEDDS), Eur. J. Pharm. Biopharm. 72 (2009) 539–545.
[16] D. Patel, K.K. Sawant, Self microemulsifying drug delivery system: formulation development and biopharmaceutical evaluation of lipophilic drugs, Curr. Drug Deliv. 6 (2009) 419–424.

[17] K. Sigfridsson, A. Lundgvist, M. Strimfors, Co-administration of a nanosuspension of a poorly soluble basic compound and a solution of a proton pump inhibitor—the importance of gastrointestinal pH and solubility for the in vivo exposure, Drug Dev. Ind. Pharm. 37 (2011) 1036–1042.
[18] K.S. Sigfridsson, A. Nordmark, S. Theilig, A. Lindahl, A formulation comparison between micro- and nanosuspensions: the importance of particle size for absorption of a model compound, following repeated oral administration to rats during early development, Drug Dev. Ind. Pharm. 37 (2011) 185–192.
[19] A.M. Cerdeira, M. Mazzoti, B. Gander, Miconazole nanosuspensions: influence of formulation variables on particle size reduction and physical stability, Int. J. Pharm. 396 (2010) 210–218.
[20] W. Li, Y. Yang, Y. Tian, X. Xu, Y. Chen, L. Mu, Y. Zhang, L. Fang, Preparation and in vitro/in vivo evaluation of revaprazan hydrochloride nanosuspension, Int. J. Pharm. 408 (2011) 157–162.
[21] P. Kayaert, G. Van den Mooter, Is the amorphous fraction of a dried nanosuspension caused by milling or by drying? A case study with naproxen and cinnarizine, Eur. J. Pharm. Biopharm. 81 (2012) 650–656.
[22] S. Bolton, Optmization techniques in pharmaceutical statistics: practical and clinical applications, Marcel Dekker, Inc., New York, 1997.
[23] B. Singh, R. Kumar, N. Ahuja, Optimizing drug delivery systems using systematic "design of experiments". Part I: fundamental aspects, Crit. Rev. Ther. Drug Carrier Syst. 22 (2005) 27–105.
[24] M. Ringnér, What is principal component analysis? Nat. Biotechnol. 26 (2008) 303–304.
[25] T. Rajalahti, O.M. Kvalheim, Multivariate data analysis in pharmaceutics: a tutorial review, Int. J. Pharm. 417 (2011) 280–290.
[26] K. Garala, J. Patel, A. Patel, A. Dharamsi, Enhanced encapsulation of metoprolol tartrate with carbon nanotubes as adsorbent, Appl. Nanosci. 1 (2011) 219–230.
[27] R. Ambrus, P. Kocbek, J. Kristl, R. Sibanc, R. Rajkó, P. Szabó-Révész, Investigation of preparation parameters to improve the dissolution of poorly water-soluble meloxicam, Int. J. Pharm. 381 (2009) 153–159.
[28] I. Ghosh, S. Bose, R. Vippagunta, F. Harmon, Nanosuspension for improving the bioavailability of a poorly soluble drug and screening of stabilizing agents to inhibit crystal growth, Int. J. Pharm. 409 (2011) 260–268.
[29] M. Nakarani, P. Patel, J. Patel, Cyclosporine nanosuspension: formulation, characterization and in vivo comparison with a marketed formulation, Sciatica Pharm. 78 (2010) 345–361.
[30] V. Teeranachaideekul, V.B. Junyaprasert, E.B. Souto, R.H. Muller, Development of ascorbyl palmitate nanocrystals applying the nanosuspension technology, Int. J. Pharm. 354 (2008) 227–234.
[31] K.K. Singh, K.K. Srinivasan, K. Gowthamarajan, D.S. Singare, D. Prakash, N.B. Gaikwad, Investigation of preparation parameters of nanosuspension by top–down media milling to improve the dissolution of poorly water-soluble glyburide, Eur. J. Pharm. Biopharm. 78 (2011) 441–446.
[32] M. Kakran, R. Shegokar, N.G. Sahoo, S. Gohla, L. Li, R.H. Müller, Long-term stability of quercetin nanocrystals prepared by different methods, J. Pharm. Pharmacol. 4 (2012) 1394–1402.
[33] Y. Gao, Z. Li, M. Sun, C. Guo, A. Yu, Y. Xi, J. Cui, H. Lou, G. Zhai, Preparation and characterization of intravenously injectable curcumin nanosuspension, Drug Deliv. 18 (2011) 131–142.
[34] P. Costa, J.M.S. Lobo, Modeling and comparison of dissolution profiles, Eur. J. Pharm. 13 (2001) 123–133.
[35] S. Bose, D. Schenck, I. Ghosh, A. Hollywood, E. Maulit, C. Ruegger, Application of spray granulation for conversion of a nanosuspension into a dry powder form, Eur. J. Pharm. 47 (2012) 35–43.
[36] Y. Wangi, Z. Liu, D. Zhang, X. Gao, X. Zhang, C. Duan, L. Jia, F. Feng, Y. Huang, Y. Shen, Q. Zhang, Development and in vitro evaluation of deacety mycoepoxydiene nanosuspension, Colloids Surf., B 83 (2011) 189–197.
[37] C.D. Hou, J.X. Wang, Y. Le, H.K. Zou, H. Zhao, Preparation of azithromycin nanosuspensions by reactive precipitation method, Drug Dev. Ind. Pharm. 38 (2012) 848–854.
[38] P. Sharma, Z.D. Zujovic, G.A. Bowmaker, W.A. Denny, S. Garg, Evaluation of a crystalline nanosuspension: polymorphism, process induced transformation and in vivo studies, Int. J. Pharm. 408 (2011) 138–151.
[39] J. Salazar, O. Heinzerling, R.H. Müller, J.P. Möschwitzer, Process optimization of a novel production method for nanosuspensions using design of experiments (DoE), Int. J. Pharm. 420 (2011) 395–403.
[40] J. Beirowski, S. Inghelbrecht, A. Arien, H. Gieseler, Freeze-drying of nanosuspensions, 1: freezing rate versus formulation design as critical factors to preserve the original particle size distribution, J. Pharm. Sci. 100 (2011) 1958–1968.
[41] P. Wang, Q. Luo, Y. Miao, L. Ying, H. He, C. Cai, X. Tang, Improved dissolution rate and bioavailability of fenofibrate pellets prepared by wet-milled-drug layering, Drug Dev. Ind. Pharm. 38 (2012) 1344–1353.
[42] G.S. Banker, Tablets, in: L. Lachman, H.A. Liberman (Eds.), The Theory and Practice of Industrial Pharmacy, 3rd ed., Varghese Publishing House, 1987, pp. 293–345.
[43] N.G. Sahoo, M. Kakran, L.A. Shaal, L. Li, R.H. Muller, M. Pal, L.P. Tan, Preparation and characterization of quercetin nanocrystals, J. Pharm. Sci. 100 (2011) 2379–2390.
[44] S. Gahoi, G.K. Jain, R. Tripathi, S.K. Pandey, M. Anwar, M.H. Warsi, M. Singhal, R.K. Khar, F.J. Ahmad, Enhanced antimalarial activity of lumefantrine nanopowder prepared by wet-milling DYNO MILL technique, Colloids Surf., B 95 (2012) 16–22.
[45] S. Basa, T. Muniyappan, P. Karatgi, R. Prabhu, R. Pillai, Production and in vitro characterization of solid dosage form incorporating drug nanoparticles, Drug Dev. Ind. Pharm. 34 (2008) 1209–1218.
[46] Indian Pharmacopoeia (IP), The Controller of Publication, New Delhi, 2010.
[47] V. Nekkanti, R. Pillai, V. Venkateshwarlu, T. Harisudhan, Development and characterization of solid oral dosage form incorporating candesartan nanoparticles, Pharm. Dev. Technol. 14 (2009) 290–298.
[48] L. Jonghwi, Drug nano- and microparticles processed into solid dosage forms: physical properties, J. Pharm. Sci. 92 (2003) 2057–2068.
[49] J. Chingunpitak, S. Puttipipatkahchorn, P. Chavallitshewinkoon-Petmitr, Y. Tozuka, K. Moribe, K. Yamamoto, Formation, physical stability and in vitro antimalarial activity of dihydroartemisinin nanosuspensions obtained by co-grinding method, Drug Dev. Ind. Pharm. 34 (2008) 314–322.
[50] P. Liu, X. Rong, J. Laru, B. Van Veen, J. Kievaara, J. Hirvonen, T. Laaksonen, L. Peltonen, Nanosuspensions of poorly soluble drugs: preparation and development by wet milling, Int. J. Pharm. 411 (2011) 215–222.
[51] M.N. Ghosh, Fundamentals of Experimental Pharmacology, 3rd ed. SK Ghosh & Others, Calcutta, India, 2008.
[52] X. Wu, J. Xu, X. Huang, C. Wen, Self-microemulsifying drug delivery system improves curcumin dissolution and bioavailability, Drug Dev. Ind. Pharm. 37 (2011) 15–23.
[53] D.M. Brahmankar, B.S. Jaiswal, Biopharmaceutics and Pharmacokinetics: A treatise, 1st ed. Vallabh Prakashan, New Delhi, 1987.
[54] A.R. Dixit, S.J. Rajput, S.G. Patel, Preparation and bioavailability assessment of SMEDDS containing valsartan, AAPS PharmSciTech 11 (2010) 314–321.
[55] D. Xia, P. Quan, H. Piao, H. Piao, S. Sun, Y. Yin, F. Cui, Preparation of stable nitrendipine nanosuspensions using the precipitation–ultrasonication method for enhancement of dissolution and oral bioavailability, Eur. J. Pharm. 40 (2010) 325–334.
[56] M. Sun, L. Si, X. Zhai, Z. Fan, Y. Ma, R. Zhang, X. Yang, The influence of co-solvents on the stability and bioavailability of rapamycin formulated in self-microemulsifying drug delivery systems, Drug Dev. Ind. Pharm. 37 (2011) 986–994.
[57] A. Dolenc, J. Kristl, S. Baumgartner, O. Planinsek, Advantages of celecoxib nanosuspension formulation and transformation into tablets, Int. J. Pharm. 376 (2009) 204–212.
[58] A. Bhakay, M. Merwade, E. Bilgili, R.N. Dave, Novel aspects of wet milling for the production of microsuspensions and nanosuspensions of poorly water soluble drugs, Drug Dev. Ind. Pharm. 37 (2011) 963–976.
[59] D.S. Singare, S. Marella, K. Gowthamrajan, G.T. Kulkarni, R. Vooturia, P.S. Rao, Optimization of formulation and process variable of nanosuspension: an industrial perspective, Int. J. Pharm. 402 (2010) 213–220.
[60] B. Van Eerdenbrugh, J. Vermant, J.A. Martens, L. Froyen, J. Van Humbeeck, P. Augustijns, G. Van den Mooter, A screening study of surface stabilization during the production of drug nanocrystals, J. Pharm. Sci. 98 (2009) 2091–2103.
[61] J. Lee, J.Y. Choi, C.H. Park, Characteristics of polymers enabling nanocomminution of water-insoluble drugs, Int. J. Pharm. 355 (2008) 328–336.
[62] S. Ganta, J. Paxton, B.C. Baguley, S. Garg, Formulation and pharmacokinetic evaluation of an asulacrine nanocrystalline suspension for intravenous delivery, Int. J. Pharm. 367 (2009) 179–186.
[63] D. Zhang, T. Tan, L. Gao, W. Zhao, P. Wang, Preparation of azithromycin nanosuspensions by high pressure homogenization and its physicochemical characteristics studies, Drug Dev. Ind. Pharm. 33 (2007) 569–575.
[64] R.H. Muller, C. Jacobs, Production and characterization of a budesonide nanosuspension for pulmonary administration, Pharm. Res. 19 (2002) 189–194.
[65] J. Deng, L. Huang, F. Liu, Understanding the structure and stability of paclitaxel nanocrystals, Int. J. Pharm. 390 (2010) 242–249